JOURNAL OF SCIENCE AND EDUCATION, VOLUME 66, ISSUE 2 (2026) 62-68

TẠP CHÍ KHOA HỌC VÀ GIÁO DỤC
ISSN: 1859-1612
Journal homepage: https://tckhgd.dhsphue.edu.vn

The near-zero dispersion in $CHCL_3$-infiltrated photonic crystal fibres with flower-core

Nguyen Thi Thuy[1], Pham Viet Tuan[1], Le Tran Uyen Tu[2], Nguyen Thi Oanh[1], Hoang Trong Duc[1]

[1]*University of Education, Hue University*

[2]*University of Science, Hue University*

ARTICLE INFO

Article history:
Received: 07 August 2023
Received in revised form: 28 August 2023
Accepted: 05 October 2023
Published: 20 April 2026

Keywords:
Photonic crystal fibers;
Chloroform;
Near-zero dispersion;
Supercontinuum generation.

ABSTRACT

In this paper, we present for the first time a new photonic crystal fiber with a flower-shaped hollow core of six smaller petals arranged in a circular fashion, infiltrated with chloroform. In addition, the air hole's size of the first layer is set to be smaller than that of the others in the cladding. This efficient design dramatically improves the dispersion properties of the fibers. Two near-zero ultra-flat dispersions with small fluctuations are obtained, values of ±0.996 ps/nm.km in the wavelength region of 1439 nm − 1698 nm, and ±1.159 ps/nm.km in the wavelength region of 569 nm − 1861 nm, respectively. These PCFs are new layers of fibers, replacing the previous glass-core fibers, suitable for small-power supercontinuum generation applications.

1. INTRODUCTION

With the flexibility in structural design leading to a good guide of light modes, photonic crystal fibers (PCFs) have attracted the attention of research groups around the world. The variation in the shape, size, and position of the air holes in the cladding along the propagation length with the correct selection of the base material allows to control dispersion, transmission, and even the nonlinear properties of the fibers (Agrawal, 2013). Thus, PCFs become excellent nonlinear means for supercontinuum (SC) generation (Dudley et al., 2006). The extremely continuous expansion of output pulses as the intense laser pulse propagates in nonlinear media makes SC suitable for many fields of applications in optical communication, biomedical sensing, spectroscopy, frequency metrology, tomography, and multimodal biophotonic imaging (Jia et al., 2022; Cruz et al., 2015; Fortier & Baumann, 2019; Cui et al., 2017).

If the laser pulse propagates in an anomalous dispersion regime, the existence of higher-order dispersion and the influence of nonlinear effects including effective mode area, nonlinear coefficients lead to the separation of higher-order solitons from fundamental solitons. As a result, new wavelengths are created, the spectrum is continuously broadened, and bandwidth is enhanced. Unfortunately, the spectrum is often restricted to the red wavelength region because of the large effective mode area in this region. Similarly, when all-normal dispersion PCFs are used for SC generation, the self-phase modulation followed by optical wave breaking are the main mechanisms for SC spectrum expansion but the bandwidth is also often limited on the red wavelength side. Therefore, optimizing the design to obtain a suitable effective mode area to expand the SC spectrum further is also one of the goals of the studies.

It is a real challenge to design modern photonic crystals and fabricate them (Mahdiraji et al., 2014). Although the creativity in the design of PCFs structures is unlimited, some geometries can cause experimental and fabricated complexity (Alam et al., 2021). Therefore, a PCF with a relatively simple design in terms of

Corresponding author: Nguyen Thi Thuy;
E-mail: ntthuy@hueuni.edu.vn
DOI: https://doi.org/10.26459/jse.043.2026

geometry, materials as well as the size of the air hole layers in the cladding requires an intensive and knowledgeable optimization process. Many works have also verified such PCFs experimentally (Hoang et al., 2019; Hoang et al., 2020; Hoang et al., 2018).

Although $CHCl_3$ is a liquid with some interesting properties, only a few publications (Zhang et al., 2010; Wang et al., 2017; Chu et al., 2019; Thi & Van, 2023) use it to infiltrate PCF to date. Compared to fused silica, its nonlinearity ($n_2 = 1.64\times10^{-19}$ $m^2.W^{-1}$) (Chemnitz et al., 2018) is one order of magnitude higher. This allows light modes to be better confined to the core. Besides, its toxicity is lower than that of carbon disulfide and toluene (Aviado, 2017) ensuring safety in practical applications of PCF.

In this study, we propose a completely new PCF structure, the layers of air holes in the cladding are arranged in a regular hexagonal shape with the diameter of the first layer being smaller. The core is designed in a flower pattern with six small evenly spaced petals. Together with the infiltration of chloroform ($CHCl_3$), the dispersion properties of the fiber were significantly improved due to the large difference in the effective refractive index between the core and the cladding. Two near-zero ultra-flat dispersions are obtained with oscillation values of ±0.996 ps/nm.km and ±1.159 ps/nm.km in the wavelength range 1439 nm − 1698 nm, 569 nm − 1861 nm, respectively. Together with very small dispersion values at the pump wavelengths, the proposed fibers are perfectly suitable for broadband SC generation.

2. NUMERICAL MODELING OF THE PCFs

Due to the diversity in the design of structures for PCFs, the Lumerical Mode Solution software (LMS) is chosen to model the hollow core PCF structures infiltrated with $CHCl_3$. The background material of the cladding is fused silica (SiO_2), which is entered into the data system by declaring the Sellmeier coefficients of the refractive index according to equation (1) (Kedenburg et al., 2012). The eight rings of air holes in the cladding are regularly arranged in a hexagonal fashion, parallel to the axis of the core. The first ring consists of six smaller air holes with a diameter of d_1. The air holes of the second to eighth rings are larger in diameter d_2. The idea of designing PCFs that emphasize the difference in the size of the air holes in the rings of the cladding comes from the works (Thi et al., 2022; Thi et al., 2023a; Thi et al., 2023b; Saitoh et al., 2006; Stępniewski et al., 2018) which verified that: The air hole's size in the first ring has a great role in controlling dispersion efficiency including flatness, preferred, slope and zero dispersion wavelength shift (ZDW). The remaining rings strongly affect the nonlinear properties of the fiber, especially the loss in the fundamental mode and even in the higher order modes. The optical properties of the PCFs in this study are investigated according to the variation of the filling factor d_1/Λ and pitch Λ (distance between adjacent air holes). The hollow-core with a diameter of D_c is the largest air hole designed in the shape of a flower with six small petals. The nonlinear liquid $CHCl_3$ is filled into the core by setting up the Sellmeier coefficients of the refractive index according to equation (2) (Tan, 1998). Table 1 presents the structural parameters for the design of PCFs.

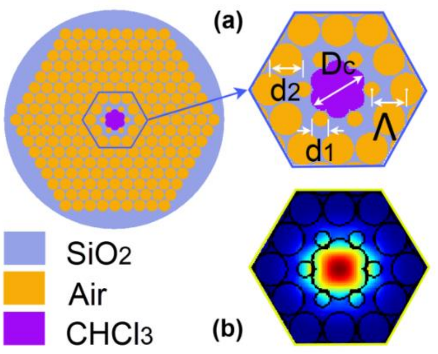

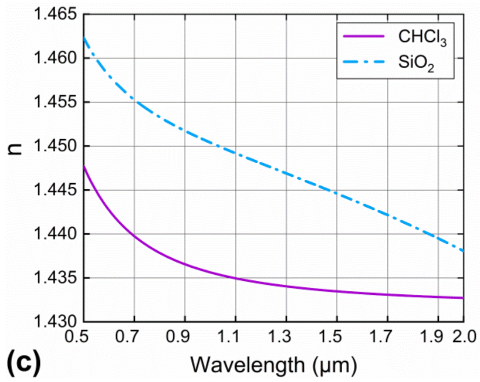

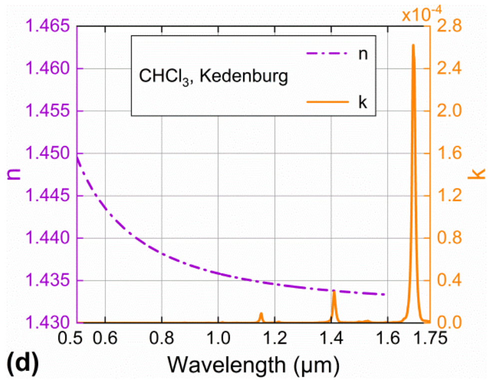

Figure 1. The cross-sections of $CHCl_3$-infiltrated PCF with flower-core (a); Light confinement in the core of PCF with Λ = 0.9 μm, d_1/Λ = 0.5 (b). The real part of the refractive index of $CHCl_3$ and fused silica is extrapolated using Sellmeier's equation (c), and the real n and imaginary k part of the refraction index of $CHCl_3$ at the temperature of 20°C is based on experimental data of Kedenburg (Kedenburg et al., 2012) (d).

$$n_{SiO_2}(\lambda)=\sqrt{1+\frac{0.6961663\lambda^2}{\lambda^2-4.679148\times10^{-3}}+\frac{0.4079426\lambda^2}{\lambda^2-1.3512063\times10^{-2}}+\frac{0.8974794\lambda^2}{\lambda^2-97.93400254}} \quad (1).$$

$$n_{CHCl_3}(\lambda)=\sqrt{1+\frac{1.04647\lambda^2}{\lambda^2-0.01048}+\frac{0.00345\lambda^2}{\lambda^2-0.15207}} \quad (2),$$

where λ is the excitation wavelength in micrometers, $n(\lambda)$ is the wavelength-dependent linear refractive index of materials.

Table 1. The structural parameters for the design of PCFs

	Λ = 0.8 (µm)			Λ = 0.9 (µm)		
d_1/Λ	d_1 (µm)	d_2 (µm)	D_c (µm)	d_1 (µm)	d_2 (µm)	D_c (µm)
0.3	0.24	0.76	1.492	0.27	0.855	1.6785
0.35	0.28	0.76	1.46	0.315	0.855	1.6425
0.45	0.36	0.76	1.384	0.405	0.855	1.557
0.5	0.4	0.76	1.34	0.45	0.855	1.5075
0.55	0.44	0.76	1.292	0.495	0.855	1.4535
0.6	0.48	0.76	1.24	0.54	0.855	1.395
0.65	0.52	0.76	1.184	0.585	0.855	1.332
	Λ = 1.5 (µm)			Λ = 2.0 (µm)		
0.3	0.45	1.425	2.7975	0.6	1.9	3.73
0.35	0.525	1.425	2.7375	0.7	1.9	3.65
0.45	0.675	1.425	2.595	0.9	1.9	3.46
0.5	0.75	1.425	2.5125	1	1.9	3.35
0.55	0.825	1.425	2.4225	1.1	1.9	3.23
0.6	0.9	1.425	2.325	1.2	1.9	3.1
0.65	0.975	1.425	2.22	1.3	1.9	2.96

To simulate electromagnetic wave propagation in PCFs, we solve numerically Maxwell's wave equations with the full vector finite difference eigencoding (FDE) method. The boundary condition is that perfectly matched layers are set up at the outermost position of the eighth ring of air holes. Hundreds of thousands of rectangles with very small areas (Yee's mesh) (Zhu & Brown, 2002) have been divided over the PCF cross-section so that the optical properties per Yee's mesh are unchanged and the propagation coefficient is calculated with high precision. The image of well-guided light modes in the cores of PCF (Λ = 0.9 µm, d_1/Λ = 0.6) is shown in figure 1b.

The dependence of the linear refractive index (the real part of the effective refractive index ($Re[n_{eff}]$) of SiO_2 and $CHCl_3$ is extrapolated by (Kedenburg et al., 2012) and verified in figure 1c. Obviously, an increase in wavelength reduces $Re[n_{eff}]$ and the real part of the effective refractive index of SiO_2 is always greater than that of $CHCl_3$, thereby determining the light-conducting mechanism as total reflection. Moreover, figure 1d also denotes the absorption spectrum of the $CHCl_3$ peak is strongest at about 1.65 µm. Therefore, in this simulation, we assume the material loss of $CHCl_3$ is equal to the value corresponding to this absorption peak.

3. SIMULATION RESULTS AND ANALYSIS

The dispersion is an important property of an optical fiber, characterized by how fast the input pulse components travel in the fiber. Dispersion depends on the wavelength (λ), the speed of light in a vacuum (c), and the effective refractive index of the guide mode, calculated by equation (3) below (Agrawal, 2013):

$$D_c=-\frac{\lambda}{c}\frac{d^2\,\mathrm{Re}[n_{eff}]}{d\lambda^2} \quad (3).$$

When Λ = 0.8 µm, the dispersion curves have a low shift below the zero dispersion with the increase of the fill factor d_1/Λ. Three anomalous dispersions with one ZDW are found with d_1/Λ = 0.3, 0.35, 0.4. Besides, ZDWs tend to move to the longer wavelength side. The all-normal dispersions include d_1/Λ = 0.45, 0.5, 0.55, 0.6. Among them, the dispersion curve with d_1/Λ = 0.45 is near-zero ultra-flat with a small value of ±0.996 ps/nm.km in the range of 259 nm. Increasing Λ to 0.9 µm, dispersion curves with d_1/Λ = 0.45, 0.5, 0.55, 0.6 gradually move upwards closer to the zero dispersion line, even intersecting the zero dispersion line at one or two points (d_1/Λ = 0.45 and 0.6) to become an anomalous dispersion curve. Among them, PCF with d_1/Λ = 0.45 has ultra-flat anomalous dispersion, flatness with ±1.159 ps/nm.km fluctuations, and covers a fairly wide wavelength region of 292 nm. As such, it becomes a near-zero hyperplane anomalous dispersion curve with the implication that this PCF can be selected to emit SC with a more extended spectrum. Continuing to increase Λ to 1.5 and 2.0 µm, the dispersion curves are all anomalous with a ZDW. When Λ is fixed, the ZDWs shift towards the short wavelength with increasing d_1/Λ.

The work (Le et al., 2018) achieved a very flat dispersion of ±1.04 ps/nm.km in the 500 nm wavelength range with ethanol-infiltrated PCF. Similarly, toluene-filled PCF in the work (Thi et al., 2023b) also showed an ultra-flattened dispersion curve with a value of ±0.947 in the 500 nm wavelength range. In the study (Duc & Thuy, 2023), the variation in dispersion over the broad wavelength range of 527 nm is ±0.753 ps/nm.km was also confirmed with benzene-filled PCF. One can also achieve near-zero dispersion for other solid-core PCFs (Maji & Chaudhuri, 2014; Kumar et al., 2020) by varying the shape and size of the air hole in all rings although that can cause production complications. Although the obtained results are also very satisfactory, the flatness and dispersion values are smaller than this work.

The ZDWs values of the $CHCl_3$-infiltrated flower-core PCFs with various d_1/Λ and Λ are displayed in table 2. The shift of the ZDW towards the short wavelength (much shorter than 1.55 µm) is not conducive to the choice of pump wavelength for SC generation. In practice, commercial laser sources have a common wavelength of 1.55 µm. It is very convenient if the pump wavelengths of the optimal PCFs have a value that matches this common pump wavelength. However, with today's diverse SC sources, that is no longer a barrier. We can use optimal PCFs to study SC generation with reasonable pump wavelength, provided they satisfy two conditions: first, the pump wavelength is chosen at a point close to the local maximum of the dispersion curve; second, it's close to ZDW.

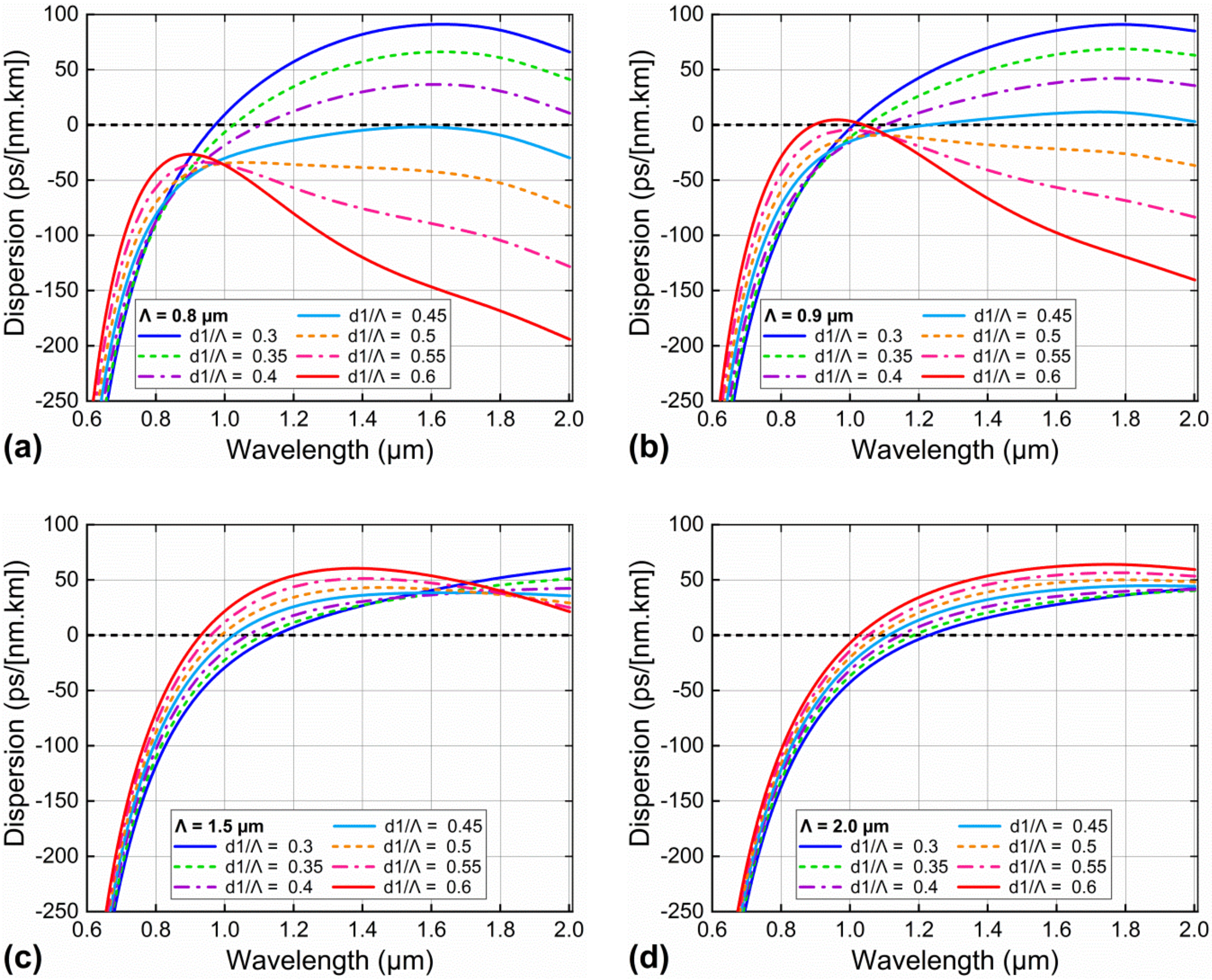

Figure 2. The dispersion of $CHCl_3$-infiltrated PCF with flower-core.

Table 2. The ZDW's value of $CHCl_3$-infiltrated flower-core PCFs with various d_1/Λ and Λ = 0.8 µm, 0.9 µm, 1.5 µm, and 2.0 µm

d_1/Λ	Λ = 0.9 µm	Λ = 0.9 µm		Λ = 1.5 µm	Λ = 2.0 µm
	ZDW_{s1}	ZDW_{s1}	ZDW_{s2}	ZDW_{s1}	ZDW_{s1}
0.3	0.971	1.01		1.146	1.227
0.35	1.024	1.048		1.111	1.184
0.4	1.104	1.1		1.066	1.145
0.45	D < 0	1.226		1.024	1.111
0.5	D < 0	D < 0		0.988	1.079
0.55	D < 0	D < 0		0.959	1.052
0.6	D < 0	0.891	1.044	0.93	1.024

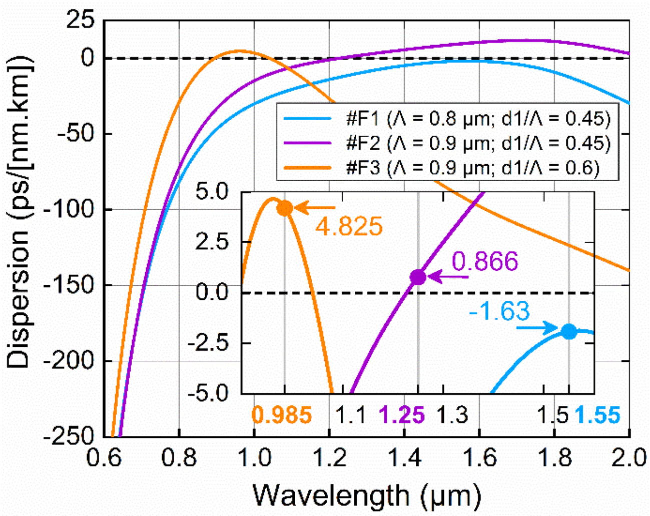

Figure 3. The dispersion properties of the three proposed fibers.

PCFs with all-normal dispersion can emit SC with a smooth, low-noise, and high-coherence spectrum thanks to the dominance of self-phase modulation and optical wave breaking. In contrast, one gets a broader spectrum, but more noisy SC based on soliton dynamics when pumping PCF in an anomalous dispersion regime. Besides, PCF with an anomalous dispersion curve has two ZDWs very close to each other, also exhibiting suppression of soliton processes even though the fiber is excited in an anomalous dispersion profile. Depending on the scope of the application, different types of fiber pumps can be proposed. Based on dispersion analyzes, we propose three optimal PCFs, with dispersion curves illustrated as shown in figure 3. #F_1 fiber (Λ = 0.8 µm and d_1/Λ = 0.45) has dispersion normal, it is recommended to pump at 1.55 µm. A rather small dispersion value of −1.63 ps/nm.km is found at this wavelength, which is suitable for the purpose of generating broad-spectrum SC with little interference. With anomalous dispersion and pump wavelength of 1.25 µm, fiber #F_2 (Λ = 0.9 µm and d_1/Λ = 0.45) has the smallest dispersion value (0.866 ps/nm.km) of the three fibers. This will help us generate SC with broad bandwidth. #F_3 fiber (Λ = 0.9 µm and d_1/Λ = 0.6) has anomalous dispersion with two very close ZDWs (ZDW_1 = 0.891 µm and ZDW_2 = 1.044 µm), which is expected for a broad SC spectrum with soliton suppression.

4. CONCLUSION

We have proposed novel structures for PCF with hollow cores infiltrated with $CHCl_3$. The combination of the flower shape of the core and the difference in the air hole size of the rings in the cladding has greatly improved the dispersion properties of the fibers. With 28 structures modeled through numerical solving of Maxwell's wave equations, we have achieved a very diverse dispersion profile, including all-normal dispersion, anomalous dispersion with one ZDW, and anomalous dispersion with two ZDWs. In particular, two near-zero ultra-flat dispersions with fluctuating flatness of ±0.996 ps/nm.km in 294 nm wavelength, and ±1,159 ps/nm.km in 432 nm wavelength are found for two fibers (Λ = 0.8 µm and d_1/Λ = 0.45; Λ = 0.9 µm and d_1/Λ = 0.45). Together with very small dispersion values at the respective pump wavelengths, the proposed fibers will be an effective new SC emitter replacing the traditional glass core fibers.

Acknowledgment. This research is funded by University of Education, Hue University under grant number NCM. T.23–02.

REFERENCES

Agrawal, G. P. (2013). *Nonlinear fiber optics* (5th ed.). Academic Press. https://doi.org/10.1016/C2011-0-00045-5

Alam, M. Z., Tahmid, M. I., Mouna, S. T., Islam, M. A., & Alam, M. S. (2021). Design of a novel star type photonic crystal fiber for mid-infrared supercontinuum generation. *Optics Communications, 500,* 127322. https://doi.org/10.1016/j.optcom.2021.127322

Aviado, D. M. (2017). *Methyl chloroform and trichloroethylene in the environment* (1st ed.). CRC Press. https://doi.org/10.1201/9781351074506

Chemnitz, M., Gaida, C., Gebhardt, M., Stutzki, F., Kobelke, J., Tünnermann, A., Limpert, J., & Schmidt, M. A. (2018). Carbon chloride-core fibers for soliton mediated supercontinuum generation. *Optics Express*, *26*(3), 3221–3235. https://doi.org/10.1364/OE.26.003221

Chu, V. L., Hoang, V. T., Long, V. C., Borzycki, K., Xuan, K. D., Quoc, V. T., Trippenbach, M., Buczyński, R., & Pniewski, J. (2019). Optimization of optical properties of photonic crystal fibers infiltrated with chloroform for supercontinuum generation. *Laser Physics*, *29*(7), 075107. https://doi.org/10.1088/1555-6611/ab2115

Cruz, F. C., Maser, D. L., Johnson, T., Ycas, G., Klose, A., Giorgetta, F. R., Coddington, I., & Diddams, S. A. (2015). Mid-infrared optical frequency combs based on difference frequency generation for molecular spectroscopy. *Optics Express, 23*(20), 26814–26824. https://doi.org/10.1364/OE.23.026814

Cui, Q., Chen, Z., Liu, Q., Zhang, Z., Luo, Q., & Fu, L. (2017). Visible continuum pulses based on enhanced dispersive wave generation for endogenous fluorescence imaging. *Biomedical Optics Express*, *8*(9), 4026–4036. https://doi.org/10.1364/BOE.8.004026

Duc, H. T., & Thuy, N. T. (2023). An ultra-flattened chromatic dispersion in circular C6H6-infiltrated photonic crystal fibers. *VNUHCM Journal of Science and Technology Development*, *26*(2), 1–13. https://doi.org/10.32508/stdj.v26i2.4074

Dudley, J. M., Genty, G., & Coen, S. (2006). Supercontinuum generation in photonic crystal fiber. *Reviews of Modern Physics*, *78*, 1135–1184. https://doi.org/10.1103/RevModPhys.78.1135

Fortier, T., & Baumann, E. (2019). 20 years of developments in optical frequency comb technology and applications. *Communications Physics, 2*, Article 153. https://doi.org/10.1038/s42005-019-0249-y

Hoang, V. T., Kasztelanic, R., Anuszkiewicz, A., Stepniewski, G., Filipkowski, A., Ertman, S., Pysz, D., Wolinski, T., Xuan, K. D., Klimczak, M., & Buczynski, R. (2018). All-normal dispersion supercontinuum generation in photonic crystal fibers with large hollow cores infiltrated with toluene. *Optical Materials Express, 8*(11), 3568–3582. https://doi.org/10.1364/OME.8.003568

Hoang, V. T., Kasztelanic, R., Filipkowski, A., Stępniewski, G., Pysz, D., Klimczak, M., Ertman, S., Long, V. C., Woliński, T. R., Trippenbach, M., Xuan, K. D., Śmietana, M., & Buczyński, R. (2019). Supercontinuum generation in an all-normal dispersion large core photonic crystal fiber infiltrated with carbon tetrachloride. *Optical Materials Express*, *9*(5), 2264–2278. https://doi.org/10.1364/OME.9.002264

Hoang, V. T., Kasztelanic, R., Stępniewski, G., Xuan, K. D., Long, V. C., Trippenbach, M., Klimczak, M., Buczyński, R., & Pniewski, J. (2020). Femtosecond supercontinuum generation around 1560 nm in hollow-core photonic crystal fibers filled with carbon tetrachloride. *Applied Optics*, *59*(12), 3720–3725. https://doi.org/10.1364/AO.385003

Jia, J., Kang, Z., Huang, Q., & He, S. (2022). Mid-infrared highly efficient, broadband, and flattened dispersive wave generation via dual-coupled thin-film lithium-niobate-on-insulator waveguide. *Applied Sciences, 12*(18), 9130. https://doi.org/10.3390/app12189130

Kedenburg, S., Vieweg, M., Gissibl, T., & Giessen, H. (2012). Linear refractive index and absorption measurements of nonlinear optical liquids in the visible and near-infrared spectral region. *Optical Materials Express, 2*(11), 1588–1611. https://doi.org/10.1364/OME.2.001588

Kumar, P., Fiaboe, K. F., & Roy, J. S. (2020). Design of nonlinear photonic crystal fibers with ultra-flattened zero dispersion for supercontinuum generation. *ETRI Journal*, *42*(2), 282–291. https://doi.org/10.4218/etrij.2019-0024

Le, H. V., Cao, V. L., Nguyen, H. T., Nguyen, A. M., Buczyński, R., & Kasztelanic, R. (2018). Application of ethanol infiltration for ultra-flattened normal dispersion in fused silica photonic crystal fibers. *Laser Physics*, *28*, 115106. https://doi.org/10.1088/1555-6611/aad93a

Mahdiraji, G. A., Chow, D. M., Sandoghchi, S. R., Amirkhan, F., Dermosesian, E., Yeo, K. S., Kakaei, Z., Ghomeishi, M., Poh, S. Y., Gang, S. Y., & Adikan, F. R. M. (2014). Challenges and solutions in fabrication of silica-based photonic crystal fibers: An experimental study. *Fiber and Integrated Optics, 33*(1–2), 85–104. https://doi.org/10.1080/01468030.2013.879680

Maji, P. S., & Chaudhuri, P. R. (2014). Supercontinuum generation in ultra-flat near zero dispersion PCF with selective liquid infiltration. *Optik, 125*(20), 5986–5992. https://doi.org/10.1016/j.ijleo.2014.07.026

Saitoh, K., Florous, N. J., & Koshiba, M. (2006). Theoretical realization of holey fiber with flat chromatic dispersion and large mode area: An intriguing defected approach. *Optics Letters, 31*(1), 26–28. https://doi.org/10.1364/OL.31.000026

Stępniewski, G., Pniewski, J., Pysz, D., Cimek, J., Stępień, R., Klimczak, M., & Buczyński, R. (2018). Development of dispersion-optimized photonic crystal fibers based on heavy metal oxide glasses for broadband infrared supercontinuum generation with fiber lasers. *Sensors, 18*(12), 4127. https://doi.org/10.3390/s18124127

Tan, C. Z. (1998). Determination of refractive index of silica glass for infrared wavelengths by IR spectroscopy. *Journal of Non-Crystalline Solids, 223*(1–2), 158–163. https://doi.org/10.1016/S0022-3093(97)00438-9

Thi, T. N., & Van, L. C. (2023). Supercontinuum spectra above 2700 nm in circular lattice photonic crystal fiber infiltrated chloroform with the low peak power. *Journal of Computational Electronics*. https://doi.org/10.1007/s10825-023-02078-w

Thi, T. N., Trong, D. H., Tran, B. T. L., Van, T. D., & Van, L. C. (2022). Optimization of optical properties of toluene-core photonic crystal fibers with circle lattice for supercontinuum generation. *Journal of Optics, 51*, 678–688. https://doi.org/10.1007/s12596-021-00802-y

Thi, T. N., Trong, D. H., & Van, L. C. (2023a). Comparison of supercontinuum spectral widths in CCl4-core PCF with square and circular lattices in the claddings. *Laser Physics, 33*(5), 055102. https://doi.org/10.1088/1555-6611/acc240

Thi, T. N., Trong, D. H., & Van, L. C. (2023b). Supercontinuum generation in ultra-flattened near-zero dispersion PCF with C7H8 infiltration. *Optical and Quantum Electronics, 55*, 93. https://doi.org/10.1007/s11082-022-04351-x

Wang, C.-C., Li, W.-M., Li, N., & Wang, W.-Q. (2017). Numerical simulation of coherent visible-to-near-infrared supercontinuum generation in the CHCl3-filled photonic crystal fiber with 1.06 μm pump pulses. *Optics & Laser Technology, 88*, 215–221. https://doi.org/10.1016/j.optlastec.2016.09.020

Zhang, H., Chang, S., Yuan, J., & Huang, D. (2010). Supercontinuum generation in chloroform-filled photonic crystal fibers. *Optik, 121*(9), 783–787. https://doi.org/10.1016/j.ijleo.2008.09.026

Zhu, Z., & Brown, T. G. (2002). Full-vectorial finite-difference analysis of microstructured optical fibers. *Optics Express, 10*, 853–864. https://doi.org/10.1364/OE.10.000853

Đặc tính tán sắc gần bằng không trong sợi tinh thể quang tử lõi hình hoa được thấm đầy $CHCl_3$

Nguyễn Thị Thủy[1], Phạm Việt Tuấn[1], Lê Trần Uyên Tú[2], Nguyễn Thị Oanh[1], Hoàng Trọng Đức[1]

[1]*Trường Đại học Sư phạm, Đại học Huế*

[2]*Trường Đại học Khoa học, Đại học Huế*

THÔNG TIN BÀI BÁO

Quá trình xử lý:
Ngày nhận bài: 07/8/2023
Ngày nhận bản chỉnh sửa: 28/8/2023
Ngày nhận đăng: 05/10/2023
Ngày xuất bản: 20/04/2026

Từ khóa:
Sợi quang tinh thể;
Chloroform;
Tán sắc gần bằng không;
Phát siêu liên tục.

Tác giả liên hệ:
Nguyễn Thị Thủy
Địa chỉ e-mail:
ntthuy@hueuni.edu.vn

TÓM TẮT

Trong bài báo này, chúng tôi lần đầu tiên đề xuất một cấu trúc sợi tinh thể quang mới với lõi rỗng hình hoa gồm sáu cánh nhỏ được sắp xếp theo hình tròn và được thấm đầy chloroform. Bên cạnh đó, kích thước các lỗ khí ở lớp thứ nhất của lớp vỏ được thiết kế nhỏ hơn so với các lỗ khí ở những lớp còn lại. Thiết kế hiệu quả này giúp cải thiện đáng kể đặc tính tán sắc của sợi. Hai cấu hình tán sắc siêu phẳng gần bằng không với độ dao động rất nhỏ đã đạt được, lần lượt là ±0,996 ps/nm·km trong dải bước sóng từ 1439 nm đến 1698 nm và ±1,159 ps/nm·km trong dải bước sóng từ 569 nm đến 1861 nm. Các sợi tinh thể quang tử này đại diện cho một thế hệ cấu trúc sợi mới, thay thế các sợi lõi thủy tinh truyền thống, phù hợp với các nguồn phát siêu liên tục công suất thấp.